FEN ve MÜHENDİSLİK BİLİMLERİ DERGİSİ

Cilt/Vol: 7 Sayı/No: 1 Yıl/Year: 2025 Araştırma Makalesi/Research Article e-ISSN: 2667-7989

https://doi.org/10.47112/neufmbd.2025.72

Titanyum Alaşımlaması ile AlCrMnV Tabanlı Hafif Yüksek Entropili Alaşımın Mikroyapı ve Sertlik Gelişimi

Tuğba Selcen ATALAY KALSEN [1*] Gökhan POLAT [2]

[1] Necmettin Erbakan University, Faculty of Engineering, Department of Metallurgical and Materials Engineering, Konya, Türkiye

[2] İzmir Katip Çelebi University, Faculty of Engineering and Architecture, Department of Metallurgy and Materials Engineering, İzmir, Türkiye

Makale Bilgisi

Geliş Tarihi: 23.01.2024
Kabul Tarihi: 24.07.2024
Yayın Tarihi: 30.04.2025

Anahtar Kelimeler:
Hafif Alaşımlar,
Mikroyapı,
Sertlik,
Yüksek Entropili Alaşımlar.

ÖZET

Yüksek entropili alaşımlar (YEA'lar), mukavemet-süneklik dengesi gibi benzersiz mekanik özellikler sergiler. Son zamanlarda hafif YEA düşük yoğunlukları ve karakteristik özellikleri nedeniyle dikkat çekmektedir. Bu çalışmada, hafif $(AlCrMnV)_{100-x}Ti_x$ (x=0, 5, 25, 50 at. %) YEA'sı içerisine Ti eklenmiş ve ark ergitme metodu ile üretilerek, Ti ilavesinin yapısal ve mekanik özelliklere etkisi incelenmiştir. Döküm numunelerin faz analizi, mikro yapıları, bileşimsel heterojenliği sırasıyla X-ışını difraktometresi (XRD), taramalı elektron mikroskobu (SEM) ve enerji dağılımlı spektrometre (EDS) ile belirlenmiştir. Döküm numunelerinin sertliği ise Vickers sertlik testiyle tespit edilmiştir. Elde edilen sonuçlara göre AlCrMnV YEAsında V-Cr ve Al-Mn açısından zengin bölgeler görülürken $(AlCrMnV)_{95}Ti_5$ YEAsında herhangi bir segregasyon gözlemlenmemiştir. Artan titanyum içeriği ile yapıya ait kafes parametresi büyüyerek, difraksiyon pikleri sola kaymasına sebep olmuştur. Titanyum içeriği at. % 0'dan at. % 25'e çıkarıldığında ise döküm numunelerinin sertliği 471 HV'den 494 HV değerine artmıştır. %5 ve %50 Ti içeren numunelerde kalıp kenarlarına yakın bölgelerde kolonsal, orta bölgelerde ise dendritik yapılar içeren ingot döküm yapıları gözlemlenmiştir. Titanyum ilavesinin $(AlCrMnV)_{100-x}Ti_x$'in mikroyapısal ve mekanik özellikleri üzerinde önemli etkisi vardır.

Microstructure and Hardness Evolution of AlCrMnV-based Lightweight High Entropy Alloy through Titanium Alloying

Article Info

Received: 23.01.2024
Accepted: 24.07.2024
Published: 30.04.2025

Keywords:
Lightweight alloys,
Microstructure,
Hardness,
High Entropy Alloy.

ABSTRACT

High-entropy alloys (HEAs) exhibit unique mechanical properties such as strength-ductility balance. Recently, light HEAs have attracted attention due to their low density and characteristic properties. In this study, Ti was gradually added to lightweight $(AlCrMnV)_{100-x}Ti_x$(x=0, 5, 25, 50 at. %) HEAs and produced by the arc melting method, and the effect of Ti addition on structural and mechanical properties was examined. Phase analysis, microstructures and compositional heterogeneity of the cast samples were determined by X-ray diffractometer (XRD), scanning electron microscope (SEM) and energy dispersive spectrometry (EDS), respectively. The hardness of the casting samples was determined by the Vickers hardness test. The results showed that V-Cr and Al-Mn rich regions were observed in the AlCrMnV sample, while no segregation was observed in the $(AlCrMnV)_{95}Ti_5$ sample. As the titanium content increased, the lattice parameter of the structure increased, causing the diffraction peaks to shift to the left. Accordingly, when the Ti content was increased from 0 at. % to 25 at. %, the hardness of the casting samples increased from 471 HV to 494 HV, respectively. Ingot cast structures, columnar at the edges, and dendritic structures, at the center zones were obtained in samples with 5 at% and 50 at.% Ti. The addition of titanium has a substantial impact on the structural and mechanical properties of $(AlCrMnV)_{100-x}Ti_x$.

To cite this article:
Atalay Kalsen, T.S. & Polat, G. (2025). Microstructure and hardness evolution of AlCrMnV-based lightweight high entropy alloy through titanium alloying. *Necmettin Erbakan University Journal of Science and Engineering, 7*(1), 22-30. https://doi.org/10.47112/neufmbd.2025.72

***Sorumlu Yazar:** Tuğba Selcen Atalay Kalsen, *tsatalay@erbakan.edu.tr*

INTRODUCTION

The concepts of high entropy alloys (HEAs) or multi-principal elements alloys (MPEAs) were first introduced and defined in 2004 by Cantor et al.[1] and Yeh et al. [2] as alloys consisting of at least five principle elements causing large configurational entropy values. These alloys can also be broadly defined as solid solution alloys, including equiatomic or near equiatomic concentration [2,3]. Although this first definition of HEAs includes the exact number and amount of the elements in the composition [4], the subsequent studies showed that this definition is restrictive and not adequate for the formation of single solid solutions [2,5]. That is, the non-equiatomic ratios and minor alloying strategy can also result in the formation of solid solution phases [6,7].

The four core effects, including high configurational entropy, lattice distortion, sluggish diffusion, and cocktail effects, are defined to reveal the influence of the different elements on the structural and mechanical properties of HEAs [6]. The application of HEAs could be expanded by tuning these basic four effects [8]. For instance, the increased number of elements can cause stable single-solid solution phases, even at elevated temperatures, due to the increased configurational entropy (ΔS_{mix}). In addition, the microstructure and mechanical properties of HEAs can be enhanced with the lower diffusion rates of the atoms, resulting from high ΔS_{mix} [9]. HEAs show high strength, hardness, high wear and corrosion resistance, high-temperature strength, and also the combination of these properties compared to conventional alloys and other materials such as composites [9–12]. Thus, HEAs have a critical role in engineering applications such as aerospace, civil transportation, catalytic, energy, biomedical, and automotive industry [6,13].

Recently, lightweight high entropy alloys (LWHEAs) having solid solution phases and enhanced properties for aerospace, transportation, and energy applications have received much attention [14,15]. Although LWHEAs consist of relatively low-density elements such as Al, Ti, Si, and Mg, the combination of Al and Ti elements with high concentrations is used to produce lightweight alloys [16–18]. Huang et al. [17] stated that Ti content significantly affects the mechanical properties of AlCrTiV alloy [17]. They also stated that increasing Ti content leads to an increase in ductility because of the reduced degree of ordering. For $Al_{10}Cr_{10}Ti_{70}V_{10}$ HEA, 877 MPa yield strength and 889 MPa ultimate tensile strength were obtained from the tensile test, according to Huang et al. [17]. Liao et al. [14] studied the effect of different amounts of V on the mechanical properties and microstructure of AlTiCrMn alloy. Accordingly, $Al_{50}(TiCrMn)_{45}V_5$ alloy showed the highest compression strength of 1995 MPa and a ductility of 30% [14].

In this study, $(AlCrMnV)_{100-x}Ti_x$ (x=0, 5, 25, 50 at. %) HEAs were prepared by vacuum arc melting, and the structural and microstructural analyses were conducted using X-ray Diffractometer (XRD) and Scanning Electron Microscope (SEM) techniques, respectively. In addition, the influence of Ti on the mechanical properties was investigated by micro Vickers tests.

MATERIALS AND METHODS

High-purity Al shots (99.9%), Ti granules (99.99%), Cr pieces (99.2%), Mn pieces (99.95%), and V pieces (99.7%) supplied from Alfa Aesar were used to produce the $(AlCrMnV)_{100-x}Ti_x$ (x=0, 5, 25, 50 at. %). The nominal compositions of the HEAs are provided in Table 1. A total metal mixture of 3 gr was prepared precisely for each set of the alloy mixture. From now on, the 0, 5, 25, and 50 at. % added HEAs were denoted as Ti0, Ti5, Ti25 and Ti50, respectively.

HEAs were produced via vacuum arc melter (Optosense, Turkey) using the current values of 130-180 A under an argon atmosphere. The ingots were remelted at least three times to ensure chemical homogeneity in the alloys. Then, the ingots were suction cast into a water-cooled cylindrical copper mold with 5 mm diameter. The cylindrical samples were mounted vertically in polyester resin to

Table 1
Nomenclatures of Samples and Concentration of Elements

HEAs	Al (at. %)	Cr (at. %)	Mn (at. %)	V (at. %)	Ti (at. %)
Ti0	25.00	25.00	25.00	25.00	-
Ti5	23.75	23.75	23.75	23.75	5.00
Ti25	18.75	18.75	18.75	18.75	25.00
Ti50	12.50	12.50	12.50	12.50	50.00

investigate the vertical cross-sections of the HEAs. Then, conventional metallographic techniques (grinding and polishing) were performed to prepare the as-cast samples. The densities of samples were measured using the Archimedes technique setup combined with a balance (RADWAG, AS 220.R2 Plus).

Phase analysis of as-cast HEAs was performed via PANalytical EMPYREAN X-ray diffractometer with Cu-Kα radiation with 0.01 step size between 10 and 100 degrees at a scanning rate of 1°/min. Hardness values of polished HEAs were obtained using the Vickers microhardness test (Emcotest, Durascan G5) under 0.5 kgf and ten seconds of indentation duration. The hardness values representing the mechanical properties [19] of the HEAs taken from five different points were used as the average hardness for each sample. The microstructure of samples was examined before and after the etching process to detect reactive phases. Etching was carried out with a solution of 5 mL HF, 4 mL HNO_3, and 65 mL H_2O for 1 min etching duration. Imaging and compositional analysis were performed via scanning electron microscope (SEM) with a tungsten filament (HITACHI, SU1510) and energy dispersive spectrometer (EDS) (Oxford Instruments, X-Act).

RESULTS AND DISCUSSION

X-ray diffraction patterns of as-cast HEAs are given in Figure 1. Phases and indexed planes were labeled on the top of the peaks. Ti0 and Ti5 samples have similar patterns compared with Ti25 and Ti50 samples, as shown in Figure 1. According to Qui et al. [20], since the BCC and B2 phases have similar lattice parameters, the XRD method cannot be sufficient to distinguish the corresponding reflections. That is, the exact amount of the B2 and BCC phases in Ti0 and Ti5 HEAs cannot be determined due to the overlapping diffraction lines in the XRD technique. In the XRD pattern, only the BCC phase peaks are visible. However, studies indicate that the B2 structure is also present in the alloys of similar composition to the samples in this study [20–22]. However, since the amount of the phase formed in this study is below 3%, it may not be visible in XRD [23]. However, the peaks could be distinguishable at higher diffraction angles, as can be seen in the XRD pattern of Ti0 and Ti5 samples, which have multiple peaks around 77-80°. A zoom-in view of the peak pattern for the Ti0 sample is given in Figure 1. These findings agree well with the previous studies by Knipling et al. [24]. However, peak positions of the BCC structures were shifted towards lower angles with increasing Ti content. As can be seen in Figure 1, 2θ degrees of the diffraction peaks belonging to $(111)_{BCC}$ plane appeared at 43.11°, 42.75°, 42.10°, and 41.07° with increasing Ti content from 0 to 50 (at. %). Accordingly, the lattice parameters of BCC structures were calculated to be 2.969 Å, 2.988 Å, 3.033 Å, and 3.111 Å for the Ti contents of 0, 5, 25, 50 (at. %), respectively. This suggests that the increasing Ti content causes a systematic increase in the lattice parameters of the HEAs due to solid solution. It can be indicated that severe lattice distortion occurred with the increasing Ti content having a relatively large atomic radius.

The formation of the BCC phase was also confirmed by thermo-physical calculations [23] provided in Table 2. As can be seen in the table, the atomic size differences (δ %) of the HEAs are well below the critical value of 6.67 % to form the solid solution in HEAs. In addition, the valance electron concentration (VEC) values of the HEAs are between 4.62 and 5.25, indicating the BCC solid solution. However, the VEC value decreases up to 4.62 in the Ti50 HEA, which further stabilizes the BCC phase,

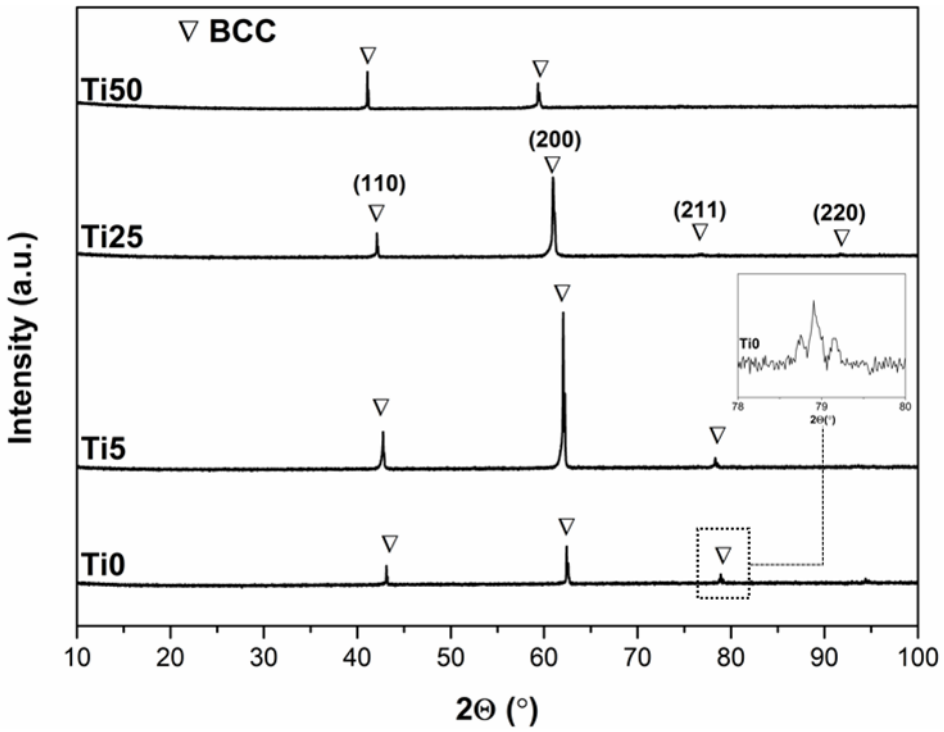

Figure 1
X-ray diffraction patterns of as-cast HEAs

and the ΔH_{mix} values of the HEAs are below the critical value of -22 kJ/mol to form solid solution phases in HEAs [25]. In addition, the thermo-physical calculation showed a decrease in the density values of the HEAs from 4.54 gr/cm^3 to 3.64 gr/cm^3 with increasing Ti. Nevertheless, the results showed the formation of solid solution phases and a decrease in the density of the HEAs with the increasing Ti content. The density values of the samples measured experimentally by Archimedes method were found to be 5.43±0.05, 5.36±0.05, 5.29±0.05, 4.94±0.03 g/cm^3 for Ti0, Ti5, Ti25, and Ti50 samples, respectively. The experimental densities of the samples show very slight deviations from the theoretical values provided in Table 2, indicating negligible porosity defects in the as-cast samples [26].

Table 2
Calculated thermo-physical properties of the HEAs

HEA	*Density (g/cm^3)*	*δ (%)*	*ΔH_{mix} (kJ/mol)*	*VEC*	*ΔS_{mix} (kJ/mol.K)*	*T_m (K)*	*VEC Predicted Phase(s)*
Ti0	5.6	4.54	-11.50	5.25	11.53	1686	BCC
Ti5	5.5	4.49	-12.61	5.19	12.60	1698	BCC
Ti25	5.3	4.20	-15.28	4.94	13.32	1748	BCC
Ti50	5.0	3.64	-14.62	4.62	11.53	1810	BCC

EDS mapping was conducted on the Ti0 and Ti5 HEAs to reveal the elemental distribution in the microstructure of Ti-free and Ti-added unetched samples. Figure 2 shows Ti0 HEA has two main regions, including Al-Mn rich and Cr-V rich phases. The segregation could be explained by mixing enthalpy (ΔH_{mix}) values of binary systems using Miedema's model [27,28]. According to Table 3, the mixing enthalpy of the Cr-V pair is -2 kJ/mol, indicating the formation of Cr-V solid solution phases in the matrix. However, the mixing enthalpy of the Al-Mn pair is -19 kJ/mol, which triggers the formation of Al-Mn intermetallic compounds (ICs).

Similarly, Son et al. [21] determined that Cr-V segregation occurred due to the mixing enthalpy in $Al_{50}VCr$ alloy. However, the distributions of the elements are more homogenous in Ti5 HEA, as seen

in Figure 2. Huang et al. [29] stated that Ti -V and Cr-V are miscible couples and Ti- Cr can dissolve in each other to form a solid solution. In addition, Al has a wide range of solubility in Ti, Cr, and V elements [29]. Therefore, the Ti5 sample has a relatively more homogeneous structure regarding elemental dispersion than Ti-free samples. These results are in line with the EDS mapping provided in Figure 2.

The HEAs were etched for detailed microstructural analyses and investigated using secondary electrons (SE) under SEM from the surface of the samples close to the mold and up to its center. Figure 3 showed SEM images taken from the overall (up to center from the surface), edge, and center regions of etched Ti5 and Ti50 samples. Cooling gradient during solidification caused ingot cast structure across both materials, as seen in Figures 3b and 3e. Columnar structures were seen at the edge of the Ti5 and Ti50 samples, while dendritic structures were formed at the center regions of the samples.

Similar microstructural features were observed by Cao et al. [30] with the addition of the V into $CoCrFeNiV_x$ (x = 0, 0.25, 0.5, 0.7, 0.8, 0.9, and 1.0). They showed the transformation of dendritic structure to distinct equiaxed grains with 0.9-1.0 V addition, which is in line with the current study.

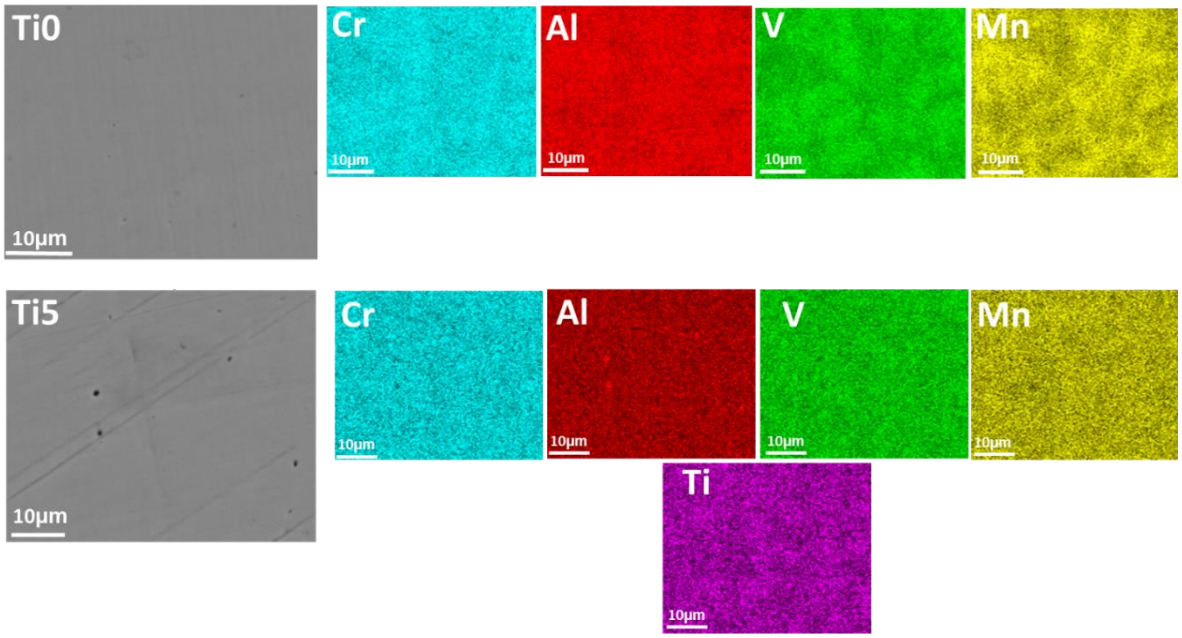

Figure 2
X-ray diffraction patterns of as-cast HEAs

Table 3
ΔH_{mix} values for atomic pairs calculated with Miedema's Model [28]

	Al	Cr	Mn	V	Ti
Al	0	-10	-19	-16	-30
Cr		0	2	-2	-7
Mn			0	-1	-8
V				0	-2
Ti					0

The chemical composition of the as-cast HEAs obtained by the EDS method is given in Table 4. It can be seen that the Al, Cr, and V contents have almost the same atomic ratios as indicated in Table 1. However, although similar amounts of Mn with Al, Cr, and V were expected in the composition, it is well below these critical ratios. This indicates the depletion of Mn in the microstructure, which can be due to the oxidation of the Mn with the trace amount of oxygen in the melting system.

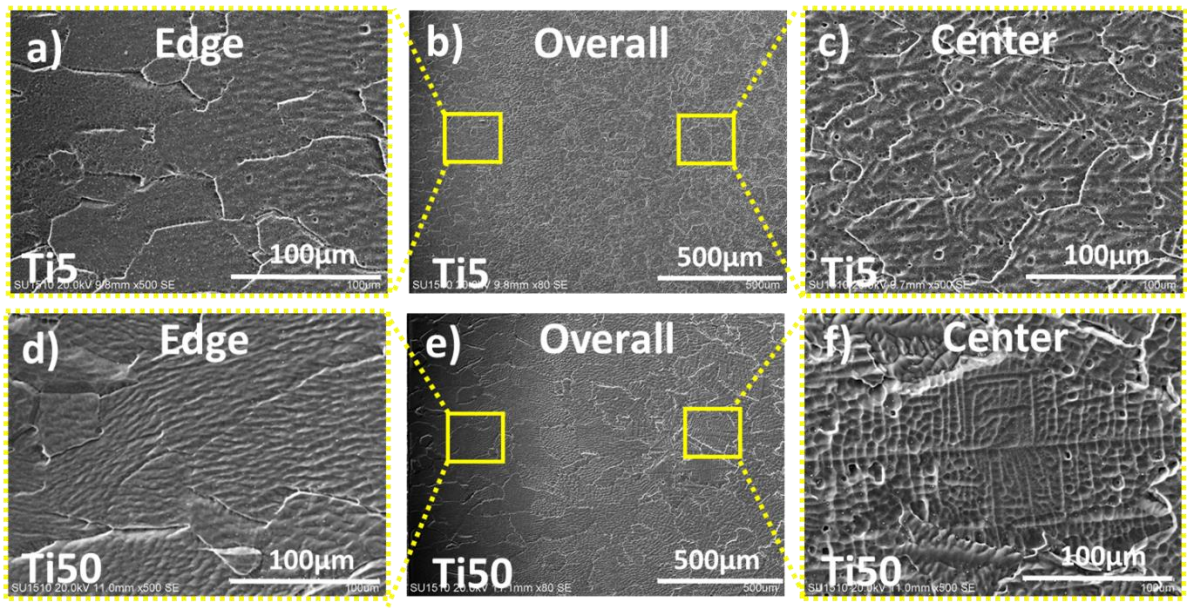

Figure 3

SEM images of etched a) Edge of Ti5 (500x), b) Overall structure of Ti5 (80x), c) Center of Ti5 (500x), d) Edge of Ti50 (500x), e) Overall structure of Ti50 (80x), f) Center of Ti50 (500x).

Table 4

Chemical composition of HEAs obtained by EDS (without etching)

	at. %			
Element	**Ti0**	**Ti5**	**Ti25**	**Ti50**
Al	27.18	24.79	18.98	12.84
Cr	27.27	24.53	18.31	12.27
Mn	17.51	19.60	17.98	12.11
V	28.04	25.07	18.41	11.74
Ti	-	6.01	26.32	51.04

The Vickers hardnesses of as-cast HEAs are given in Figure 4. Hardness values were found to be 471±7 HV, 494±5 HV, 652±4 HV, and 532±11 HV for Ti0, Ti5, Ti25 and Ti50 HEAs, respectively. That is, a systematic increase was observed in the hardness of the HEAs up to 25 at. % Ti addition. The increase in the hardness could be attributed to the increased lattice distortion of the HEAs with increasing Ti into the base (Ti0) HEA. The increasing lattice distortion could be correlated with the XRD patterns provided in Figure 1. As can be seen, the systematic addition of Ti causes a shift in the main peaks of the BCC lattice towards lower angles, indicating the expansion of the lattice

On the other hand, further increase in Ti content of 50 at. % resulted in a decrease in the hardness from 652±4 HV to 532±11 HV. The reason for the decrease in the hardness of the Ti50 HEA can be seen in Figure 1, the Ti content increased by 50%, disappearing B2 phase and causing almost a single BCC phase in the microstructure. That is, the brittle B2 phases transform into a relatively soft BCC phase, softening the hardness. Moreover, Huang et al. [17] stated that Ti has a vital role in increasing the hardness of AlCrTiV HEA. However, an excess amount of titanium in AlCrTiV alloy decreases hardness due to a reduced degree of ordering and decreasing lattice distortion. That is, as shown in Table 2, the atomic size difference of the HEAs decreases by 3.64 % in Ti50 HEA, thus triggering solid solution strengthening [17]. Nevertheless, a decrease in the hardness of the HEAs was observed in the Ti50 HEA due to formation of a relatively soft single BCC phase, and decreasing lattice distortion.

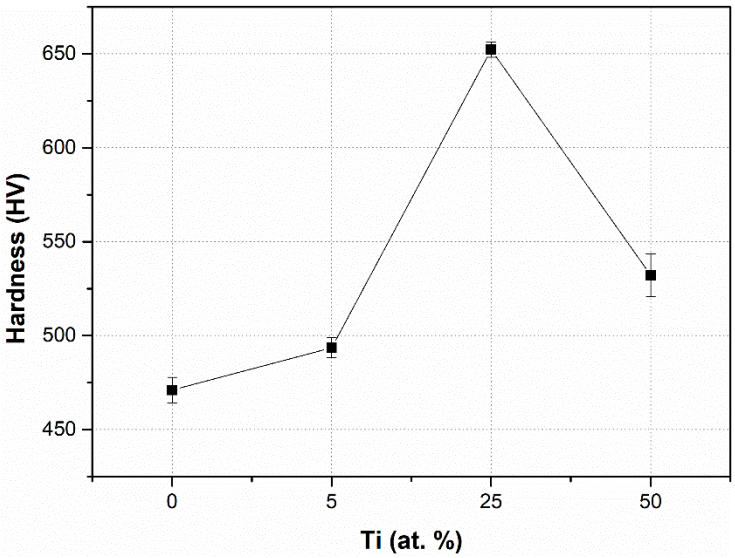

Figure 4
Ti effect on hardness of as-cast HEAs

CONCLUSIONS

In this study, 5 mm cylindrical $(AlCrMnV)_{100-x}Ti_x$ (x=0, 5, 25, 50 at. %) low-density HEAs were produced by vacuum arc melting, and the influence of Ti on the microstructural and mechanical properties was investigated. The XRD results showed the formation of the BCC phase in HEAs. The XRD analysis also indicates that the diffraction peaks of the BCC phase shifted toward the lower angles due to the increasing lattice parameter. The increasing Ti content caused a lattice distortion and increased the hardness of the HEAs. However, hardness decreased from 652 HV to 532 HV. The microstructures of HEAs were examined using SEM to investigate the cooling gradient effect. Columnar structures were found near the outer edges close to the mold, while dendritic structures were present in the central zones of the samples. The results also showed that Ti addition provided almost a homogeneous distribution of the elements in the matrix of the HEAs. In conclusion, Ti addition has a significant effect on the properties of $(AlCrMnV)_{100-x}Ti_x$ in terms of the formation of solid solution phases and tuning the corresponding mechanical properties.

Ethical Statement
This study is an original research article designed and developed by the authors.

Acknowledgements
The authors would like to thank the Necmettin Erbakan University Science and Technology Research and Application Center (BITAM) for their support in the production and characterization of alloys.

Author Contributions
Research Design (CRediT 1) T.S.A.K. (%50) - G.P. (%50)
Data Collection (CRediT 2) T.S.A.K. (%60) - G.P. (%40)
Research - Data Analysis – Validation (CRediT 3-4-6-11) T.S.A.K. (%50) - G.P. (%50)
Writing the Article (CRediT 12-13) T.S.A.K. (%60) - G.P. (%40)
Revision and Improvement of the Text (CRediT 14) T.S.A.K. (%50) - G.P. (%50)

Financing
This research was not supported by any public, commercial, or non-profit organization.

Conflict of Interest
The authors declare no conflict of interest.

REFERENCES

[1] B. Cantor, I.T.H. Chang, P. Knight, A.J.B. Vincent, Microstructural development in equiatomic multicomponent alloys, *Materials Science and Engineering: A*. 375–377 (2004), 213–218. doi:10.1016/J.MSEA.2003.10.257

[2] J.-W. Yeh, S.-K. Chen, S.-J. Lin, J.-Y. Gan, T.-S. Chin, T.-T. Shun, C.-H. Tsau, S.-Y. Chang, Nanostructured high-entropy alloys with multiple principal elements: novel alloy design concepts and outcomes, *Advanced Engineering Materials*. 6 (2004), 299–303. doi: 10.1002/adem.200300567

[3] Y. Zhang, T.T. Zuo, Z. Tang, M.C. Gao, K.A. Dahmen, P.K. Liaw, Z.P. Lu, Microstructures and properties of high-entropy alloys, *Progress in Materials Science*. 61 (2014), 1–93. doi: 10.1016/j.pmatsci.2013.10.001

[4] D.B. Miracle, O.N. Senkov, A critical review of high entropy alloys and related concepts, *Acta Materialia*. 122 (2017), 448–511. doi:10.1016/j.actamat.2016.08.081

[5] F. Otto, Y. Yang, H. Bei, E.P. George, Relative effects of enthalpy and entropy on the phase stability of equiatomic high-entropy alloys, *Acta Materialia*. 61 (2013), 2628–2638. doi: 10.1016/j.actamat.2013.01.042

[6] J.W. Yeh, Recent progress in high-entropy alloys, *Annales de Chimie Science Des Materiaux (Paris)*. 31 (2006), 633–648

[7] D. Ma, M. Yao, K.G. Pradeep, C.C. Tasan, H. Springer, D. Raabe, Phase stability of non-equiatomic CoCrFeMnNi high entropy alloys, *Acta Materialia*. 98 (2015), 288–296. doi: 10.1016/j.actamat.2015.07.030

[8] B.S. Murty, J.W. Yeh, S. Ranganathan, Chapter 2 - High-Entropy Alloys: Basic Concepts, in: B.S. Murty, J.W. Yeh, S.B.T.-H.E.A. Ranganathan (Eds.), *Butterworth-Heinemann*, Boston, 2014: pp. 13–35. doi: 10.1016/B978-0-12-800251-3.00002-X

[9] N. Nayan, G. Singh, S.V.S.N. Murty, A.K. Jha, B. Pant, K.M. George, U. Ramamurty, Hot deformation behaviour and microstructure control in AlCrCuNiFeCo high entropy alloy, *Intermetallics*. 55 (2014), 145–153. doi: 10.1016/j.intermet.2014.07.019

[10] Y.J. Zhou, Y. Zhang, Y.L. Wang, G.L. Chen, Solid solution alloys of AlCoCrFeNiTix with excellent room-temperature mechanical properties, *Applied Physics Letters*. 90 (2007), 181904. doi:10.1063/1.2734517

[11] E. Madenci, Fonksiyonel derecelendirilmiş malzeme plakların statik analizinde mikro-mekanik modellerin katkısı, *Necmettin Erbakan Üniversitesi Fen ve Mühendislik Bilimleri Dergisi*. 5 (2023), 23–37. doi:10.47112/neufmbd.2023.7

[12] L. Gemi, M. Azeem, Ş. Yazman, M. Kayrıcı, O. Gök, Investigation of mechanical properties and damage development of filament wound GFRP composite pipes by ring tensile test, *Necmettin Erbakan Üniversitesi Fen ve Mühendislik Bilimleri Dergisi*. 6 (2024), 93–104. doi:10.47112/neufmbd.2024.34

[13] E.P. George, W.A. Curtin, C.C. Tasan, High entropy alloys: A focused review of mechanical properties and deformation mechanisms, *Acta Materialia*. 188 (2020), 435–474. doi: 10.1016/j.actamat.2019.12.015

[14] Y.-C. Liao, P.-S. Chen, C.-H. Li, P.-H. Tsai, J.S.C. Jang, K.-C. Hsieh, C.-Y. Chen, P.-H. Lin, J.C. Huang, H.-J. Wu, Y.-C. Lo, C.-W. Huang, I.-Y. Tsao, Development of novel lightweight dual-phase Al-Ti-Cr-Mn-V medium-entropy alloys with high strength and ductility, *Entropy*. 22 (2020). doi:10.3390/e22010074

[15] O. Maulik, D. Kumar, S. Kumar, S.K. Dewangan, V. Kumar, Structure and properties of lightweight high entropy alloys: a brief review, *Materials Research Express*. 5 (2018), 52001. doi:10.1088/2053-1591/aabbca

[16] M.J. Chae, A. Sharma, M.C. Oh, B. Ahn, Lightweight AlCuFeMnMgTi high entropy alloy with high strength-to-density ratio processed by powder metallurgy, *Metals and Materials International*. 27 (2021), 629–638. doi:10.1007/s12540-020-00823-5

[17] X. Huang, J. Miao, A.A. Luo, Order-disorder transition and its mechanical effects in lightweight AlCrTiV high entropy alloys, *Scripta Materialia*. 210 (2022), 114462. doi: 10.1016/j.scriptamat.2021.114462

[18] K.M. Youssef, A.J. Zaddach, C. Niu, D.L. Irving, C.C. Koch, A Novel Low-Density, High-Hardness, High-entropy Alloy with Close-packed Single-phase Nanocrystalline Structures, *Materials Research Letters*. 3 (2015), 95–99. doi:10.1080/21663831.2014.985855

[19] İ. Oral, Prediction of hardness values of some wooden materials using computer-aided tap testing, *Necmettin Erbakan Üniversitesi Fen ve Mühendislik Bilimleri Dergisi*. 5 (2023), 257–266. doi:10.47112/neufmbd.2023.23

[20] [Y. Qiu, Y.J. Hu, A. Taylor, M.J. Styles, R.K.W. Marceau, A. V. Ceguerra, M.A. Gibson, Z.K. Liu, H.L. Fraser, N. Birbilis, A lightweight single-phase AlTiVCr compositionally complex alloy, *Acta Materialia*. 123 (2017), 115–124. doi:10.1016/J.ACTAMAT.2016.10.037

[21] S. Son, P. Asghari-Rad, J. Choi, A. Kim, J.-H. Jeong, S. Cho, H.S. Kim, Design and mechanical properties of body-centered cubic AlVCr medium-entropy aluminum alloys, *Journal of Materials Research and Technology*. 24 (2023), 7302–7312. doi: 10.1016/j.jmrt.2023.05.021

[22] K. Knipling, P. Narayana, L. Nguyen, D. Beaudry, Microstructures and properties of as-cast AlCrFeMnV, AlCrFeTiV, and AlCrMnTiV multi-principal element alloys, *Journal of Applied Physics*. 133 (2023), 104901. doi:10.1063/5.0135276

[23] G. Polat, Z.A. Erdal, Y.E. Kalay, Design of Novel Non-equiatomic Cu-Ni-Al-Ti Composite Medium-Entropy Alloys, *Journal of Materials Engineering and Performance*. 29 (2020), 2898–2908. doi:10.1007/s11665-020-04830-w

[24] K.E. Knipling, P.U. Narayana, L.T. Nguyen, Microstructures and properties of As-Cast AlCrFeMnV, AlCrFeTiV, and AlCrMnTiV high entropy alloys, *Microscopy and Microanalysis*. 23 (2017), 702–703. doi:10.1017/S1431927617004172

[25] S. Guo, C.T. Liu, Phase stability in high entropy alloys : Formation of solid-solution phase or amorphous phase, *Progress in Natural Science: Materials International*. 21 (2011), 433–446. doi:10.1016/S1002-0071(12)60080-X

[26] G. Polat, T.S. Atalay Kalsen, Al içeriğinin (CoCrFe)60AlxNi(40-x) Yüksek entropili alaşımının yapısal ve mekanik özellikleri üzerindeki etkisi, *Kahramanmaraş Sütçü İmam Üniversitesi Mühendislik Bilimleri Dergisi*. 26 (2023), 812–822. doi:10.17780/ksujes.1279081

[27] C. Li, Y. Yuan, F. Li, Q. Wei, Y. Huang, Modification and verification of Miedema model for predicating thermodynamic properties of binary precipitates in multi-element alloys, *Physica B: Condensed Matter*. 627 (2022), 413540. doi:10.1016/j.physb.2021.413540

[28] A. Takeuchi, A. Inoue, Classification of bulk metallic glasses by atomic size difference, heat of mixing and period of constituent elements and ıts application to characterization of the main alloying element, *Materials Transactions*. 46 (2005), 2817–2829. doi:10.2320/matertrans.46.2817

[29] X. Huang, J. Miao, A.A. Luo, Lightweight AlCrTiV high-entropy alloys with dual-phase microstructure via microalloying, *Journal of Materials Science*. 54 (2019) 2271–2277. doi:10.1007/s10853-018-2970-4

[30] L. Cao, L. Zhu, H. Shi, Z. Wang, Y. Yang, Y. Meng, L. Zhang, Y. Cui, microstructural evolution from dendrites to core-shell equiaxed grain morphology for $CoCrFeNiV_x$ high-entropy alloys in metallic casting mold, *Metals*, 9 (2019), 1172. doi:10.3390/MET9111172